energies

MDPI

Review

A Review on the Influence of CO_2/Shale Interaction on Shale Properties: Implications of CCS in Shales

Ahmed Fatah [1], Ziad Bennour [1], Hisham Ben Mahmud [1], Raoof Gholami [1] and Md. Mofazzal Hossain [2,*]

[1] Department of Petroleum Engineering, Curtin University, Miri 98009, Malaysia; a.fatah@postgrad.curtin.edu.my (A.F.); z.bennour@curtin.edu.my (Z.B.); hisham@curtin.edu.my (H.B.M.); raoof.gholami@curtin.edu.my (R.G.)

[2] Petroleum Engineering Discipline, WA School of Mines: Minerals, Energy and Chemical Engineering, Curtin University, Perth, WA 6102, Australia

* Correspondence: md.hossain@curtin.edu.au

Received: 30 April 2020; Accepted: 16 June 2020; Published: 19 June 2020

Abstract: Carbon capture and storage (CCS) is a developed technology to minimize CO_2 emissions and reduce global climate change. Currently, shale gas formations are considered as a suitable target for CO_2 sequestration projects predominantly due to their wide availability. Compared to conventional geological formations including saline aquifers and coal seams, depleted shale formations provide larger storage potential due to the high adsorption capacity of CO_2 compared to methane in the shale formation. However, the injected CO_2 causes possible geochemical interactions with the shale formation during storage applications and CO_2 enhanced shale gas recovery (ESGR) processes. The CO_2/shale interaction is a key factor for the efficiency of CO_2 storage in shale formations, as it can significantly alter the shale properties. The formation of carbonic acid from CO_2 dissolution is the main cause for the alterations in the physical, chemical and mechanical properties of the shale, which in return affects the storage capacity, pore properties, and fluid transport. Therefore, in this paper, the effect of CO_2 exposure on shale properties is comprehensively reviewed, to gain an in-depth understanding of the impact of CO_2/shale interaction on shale properties. This paper reviews the current knowledge of the CO_2/shale interactions and describes the results achieved to date. The pore structure is one of the most affected properties by CO_2/shale interactions; several scholars indicated that the differences in mineral composition for shales would result in wide variations in pore structure system. A noticeable reduction in specific surface area of shales was observed after CO_2 treatment, which in the long-term could decrease CO_2 adsorption capacity, affecting the CO_2 storage efficiency. Other factors including shale sedimentary, pressure and temperature can also alter the pore system and decrease the shale "caprock" seal efficiency. Similarly, the alteration in shales' surface chemistry and functional species after CO_2 treatment may increase the adsorption capacity of CO_2, impacting the overall storage potential in shales. Furthermore, the injection of CO_2 into shales may also influence the wetting behavior. Surface wettability is mainly affected by the presented minerals in shale, and less affected by brine salinity, temperature, organic content, and thermal maturity. Mainly, shales have strong water-wetting behavior in the presence of hydrocarbons, however, the alteration in shale's wettability towards CO_2-wet will significantly minimize CO_2 storage capacities, and affect the sealing efficiency of caprock. The CO_2/shale interactions were also found to cause noticeable degradation in shales' mechanical properties. CO_2 injection can weaken shale, decrease its brittleness and increases its plasticity and toughness. Various reductions in tri-axial compressive strength, tensile strength, and the elastic modulus of shales were observed after CO_2 injection, due to the dissolution effect and adsorption strain within the pores. Based on this review, we conclude that CO_2/shale interaction is a significant factor for the efficiency of CCS. However, due to the heterogeneity of shales, further studies are needed to include various shale formations and identify how different shales' mineralogy could affect the CO_2 storage capacity in the long-term.

Keywords: shale gas; CO_2 injection; CO_2 sequestration; CO_2 storage capacity; CO_2/shale interaction

1. Introduction

The development of carbon capture and storage (CCS) stands as a suitable technology to reduce the massive increase in CO_2 emissions in recent decades, as global climate change is becoming a serious concern to the public environment and economic growth [1]. CO_2 geological sequestration was proposed as a reliable technique to mitigate the emissions of greenhouse gas from fossil fuels into the atmosphere, by injecting CO_2 for long-term storage and enhancing gas recovery [2–4]. Conventional geological formations with high pore volume, including saline aquifers, depleted oil and gas fields, and un-minable coal seams, were utilized as suitable candidates for CCS projects [5]. However, some concerns related to these formations, including cost and long-term storage, prevent efficient CO_2 storage [6]. The trapping mechanism during CO_2 storage is usually associated with the CO_2/rock interactions in the porous medium, including CO_2 absorption, minerals dissolution, dissolution trapping, capillary trapping, rock heterogeneity and physical adsorption [7]. The trapping mechanism in deep saline aquifers, for instance, is mainly driven by structural trapping; when the injected CO_2 diffuses into the formation, it reaches the top layer due to the buoyance factor, hence CO_2 would be trapped by an impermeable caprock [1]. Coal seams that have been proven to have economic potential for CCS projects at extremely deep locations are driven by an adsorption trapping mechanism, yet the injection of CO_2 is more likely to cause high swelling rates and many environmental issues [8]. In depleted reservoirs, gas absorption and structural trapping effectively work as CO_2 trapping mechanisms. The injected CO_2 will be absorbed by the immobile residual oil causing multiple-contact miscibility [7].

1.1. Development of Shale Formations

The success in developing shale formations in recent decades has shifted attention towards shale reservoirs, and considered them as promising candidates to store CO_2 for extended periods [9], mainly because shales with their ultralow permeability play a major role as barriers or seals in a petroleum reservoir system, and also due to their wide availability worldwide [7,10–15]. The breakthrough made in technology to utilize CO_2 (instead of slick-water) in developing shale formation during drilling, fracturing, and enhanced shale gas recovery (ESGR) processes leads to minimizing many environmental issues during the operations, i.e., minimizing the amount of produced wastewater and increasing the production efficiency of gas while sequestering the adsorbed CO_2 simultaneously [16–18]. These developed technologies, including hydraulic fracturing and horizontal drilling make commercial development of shale formations possible. In the US, shale gas production has increased since 2010 from about 6.16 trillion cubic feet to exceeding 20 trillion cubic feet in 2020, and is expected to reach about 35 trillion cubic feet in 2050. Forty-nine percent of the total US gas production is expected to come from shale reservoirs by 2035 [19], securing the gas production for the upcoming decades and providing the potential for CCS projects [20,21]. As illustrated in Figure 1, CCS applications hold good promise in reducing CO_2 emissions in the coming decades, despite the increase in energy demands. However, effective utilization of depleted shale gas formations as storage sites for CO_2 can significantly contribute to minimizing CO_2 emissions, assuming good connectivity between induced and existing fractures and no pore space collapse [22].

1.2. Adsorption Capacity of CO_2 in Shales

Carbon dioxide is a non-toxic fluid that is present at the reservoir in the supercritical phase when the temperature and pressure exceed 31.8 °C and 7.38 MPa, respectively. Supercritical CO_2 ($SCCO_2$) has low viscosity and no surface tension, with a high adsorption capacity relative to methane gas (CH_4) to the shale formation [22,23]. CO_2 sorption on clay and kerogen in partially depleted wells allows the displacement of CH_4 and stores more CO_2 [24–26]. As noted by many studies [13,15,26–28],

the high CO_2 adsorption capacity is the main derive mechanism for CO_2 storage in shale formation after production phase, as injecting CO_2 continuously leads to the release of the natural pre-adsorbed CH_4 during CO_2 fracturing stimulation due to the displacement mechanism and higher chemical potential. Nuttall et al. [15] presented the adsorption isotherms between CO_2 and CH_4 in Devonian shale formations, showing stronger CO_2 adsorption than CH_4, providing the potential for CO_2 sequestration in shales (Figure 2). A study conducted by Kang et al. [7] on Barnett shales confirmed the strong adsorption capacity of CO_2, which was 5–10 times higher compared to CH_4. The adsorption of CO_2 in most shales in the US indicated a similar tendency of higher adsorption than CH_4, by 2–3 times [29]. The strong CO_2 capacity provides high storage security in shale formation due to the existence of stable in-place CH_4 in the reservoir, which can be related to the fact that five CO_2 molecules can displace one CH_4 molecule, which allows the CO_2 to occupy the porous medium, providing the potential for storage application [28]. Later research has come to a similar conclusion from measuring the adsorption behavior of CO_2 and CH_4 on different shale formations, indicating that shale formations favor adsorbing CO_2, enhancing the recovery of CH_4, preventing massive leakage risks and reducing storage costs [29–31]. Tao and Clarens [6] estimated that Marcellus shale could store a total mass of CO_2 ranging between 10.4 and 18.4 gigatonnes (Gt) (1 Gt = 10^{12} kg), offering the potential to store around 50% of CO_2 emissions in the US by 2030 [22]. Similarly, Edwards et al. [32] presented that Barnett Shale has a CO_2 storage capacity ranging between 2.1–3.1 Gt. These studies provide a strong foundation for the investigation of the feasibility of CCS projects in shale formations, confirming the high possibility of storage capacity in shale formations by multiple trapping mechanisms [6,10,32,33].

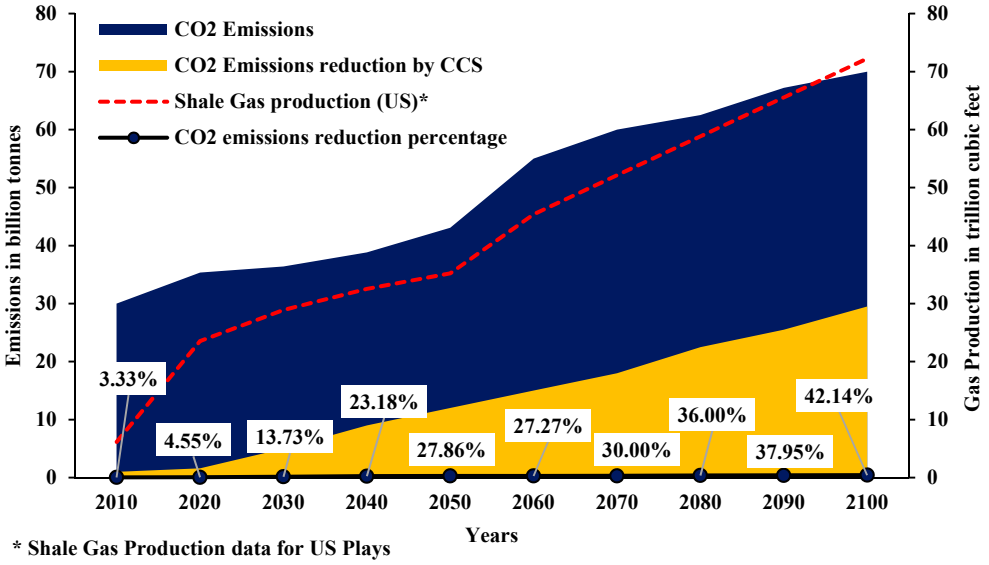

Figure 1. Carbon capture and storage (CCS) contribution percentage in CO_2 emission reduction from 2010 to 2100 [34–37].

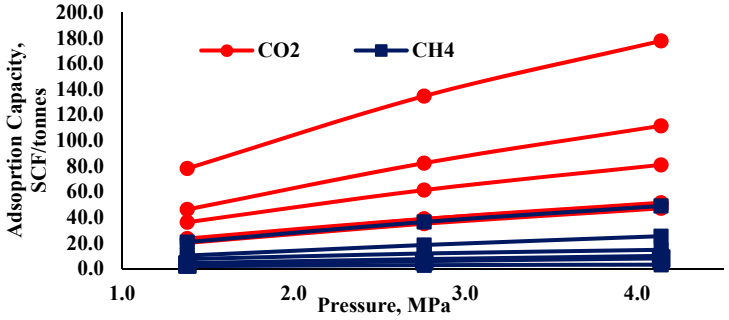

Figure 2. Adsorption capacities for CO_2 and CH_4 in Devonian shales at different pressures [15].

1.3. CCS in Shales

The injection of CO_2 into depleted shale formations may help to recover additional hydrocarbons through the ESGR process, which provides economic benefits in CCS compared to conventional storage sites. Shale formations are very promising targets for CCS, however, the rate of CO_2 injection into the shale formation should be coupled with the rate of CO_2 capture from industrial processes such as fossil fuels in power plants, ensuring the storage safety, stability and economic feasibility [4,32,33]. CO_2 is a relatively reactive substance; once injected into the shale formation, it will be trapped in the adsorbed phase. In the long-term, formation brine will dissolve the injected CO_2 and causes reactions with the shale rock, leading to mineral precipitation and dissolution which may affect the shale storage capacity [1,38]. The CO_2/shale interaction is a key factor for the efficiency of CCS in shale formations; it can significantly alter the shale properties, which in return affect the rock geometry, fluid transportation, and storage capacity [39,40]. The presence of organic and inorganic components in a heterogeneous porous medium such as shale permits the injected CO_2 to interact with clay minerals and organic matter through chemical dissolution [39]. This dissolution behavior of CO_2 can be related to the creation of carbonic acid when meeting a brine formation, leading to major changes in the shale properties [41,42].

In the last decade, enormous work was directed towards understanding the fundamentals of the CO_2–shale interaction at reservoir conditions for better CCS applications [42–52], by evaluating the impact of CO_2 injection on shales. Earlier in 2008, Busch et al. [53] found that the rock properties of Muderong shale in Australia were affected by the dissolution behavior of $SCCO_2$. These findings were supported later by several studies [54–56], confirming that $SCCO_2$ can significantly alter the pore structure system of shale, leading to changes in the porosity and the specific surface area. Some recent studies have related the effect of CO_2/shale interaction on shale properties to the mineral composition and specific reservoir conditions, including temperature, pressure, and CO_2 phase states [39,52,57,58]. However, the knowledge of CO_2–shale interaction is still evolving, and more investigations are needed to successfully apply CCS technology in shale formations technically and economically. It is crucial to address the potential interactions between CO_2 and shale formation, and their influence on CCS, to ensure the longevity of CO_2 containment [10].

In this regard, the related literature of CO_2/shale interaction and its effect on shales are comprehensively reviewed, to gain a wide understanding of the effect of CO_2 injection on shale properties. The overall assessment of CCS viability in depleted hydrocarbon shale formations depends on its reliability in terms of technical feasibility, long-term CO_2 containment and economic viability. Several studies [6,10,32,33] have supported the functionality of shales to host CO_2, related to CO_2 injectivity, storage capacity, methane gas recovery and CO_2/shale interactions. However, this paper focuses on reviewing the existing knowledge of CO_2-shale interactions and describing the results achieved to date. Therefore, the following sections address this issue and evaluate the implications of the overall storage capacity. This review also highlights the topics on Life Cycle Assessment (LCA) and the economic viability of CCS applications in shales.

2. CO_2-Shale Interaction

Long-term CO_2 sequestration in shale formations causes CO_2/shale geochemical interactions, such as mineral dissolution, gas adsorption and changes in pore structure, which affect the sealing integrity of the shale [39,53,59]. Because of the heterogeneity of shale, it is crucial to address several factors that could have a direct influence on shale properties for the specific shale formation, such as shale mineralogy, total organic carbon (TOC) content, surface morphology, geometry, pressure, and temperature [11]. This will help to evaluate the functionality of the targeted shale formation to host CO_2 for extended periods. Recently, characterization of shale formation associated with CO_2 injection has received much attention in the literature, for its importance in applying a cost-effective CCS project [60,61]. Many characterization methods, i.e., *X*-ray diffraction, scanning electron microscopy, *X*-ray fluorescence, low-pressure gas adsorption, Fourier transform infrared (FTIR) spectroscopy and

nuclear magnetic resonance (NMR) are being widely applied to investigate the effect of CO_2/shale interactions on physical and chemical properties of shales [18,39,43].

For this paper, and according to the nature of shale, the shale properties can be categorized under physical, chemical and mechanical properties; this classification is made based on the potential changes caused by CO_2 injection. This review discusses the impact of CO_2 exposure on some of the major shale properties, which are: (1) Pore structure, (2) Mineral composition, (3) Chemical properties, (4) Surface wettability and (5) Mechanical properties.

2.1. Pore Structure

The pore structure is one of the most affected properties of shale formation by CO_2 injection, therefore, any changes in pore structure may impact the efficiency of CO_2 storage capacity. This may lead to affect the economic feasibility of the CCS application. The ability of CO_2 to dissolve and extract clay minerals is the main cause of the changes in the pore morphology, this dissolution behavior of CO_2 can be attributed to the creation of carbonic acid and the chemical reaction with the formation water [41,42]. Generally, when the CO_2 is injected into the shale, it is stored as free gas in the macropores structure; over time, the CO_2–shale interaction takes place within the nanopore system, which in return affects the pore structure and its specific surface area (SSA), fractal dimension, total pore volume (TPV) and pore size distribution (PSD) [39]. Several studies have discussed the alteration of pore structure parameters when shales are exposed to CO_2, confirming that the alteration of pore structure system is affected by multiple factors including, the type of shale sedimentary, the presence of clay and non-clay mineral in the formation, and reservoir's pressure and temperature [30,39,49,50,55,56]. The alteration in the pore structure system during CO_2 injection is mainly influenced by the minerals' dissolution and precipitation. Shales are usually composed of clay minerals, quartz, carbonate, and fragments of other minerals. Several studies have characterized different shale formations and provided their typical mineral composition, as illustrated in Figure 3 [39,62–64]. Liu et al. [59] reported that the CO_2 has a limited impact on the caprock due to the miner dissolution of K-feldspar and anhydrite, along with low precipitation of illite, smectite (a mineral that contains Ca^{++} and Mg^{++}), and siderite. On the contrary, Armitage et al. [65] reported an increase in the porosity and permeability of mudstone, due to the high dissolution of chlorite and siderite by CO_2. This indicates that the differences in mineral composition for shales would result in wide variations in the pore structure system.

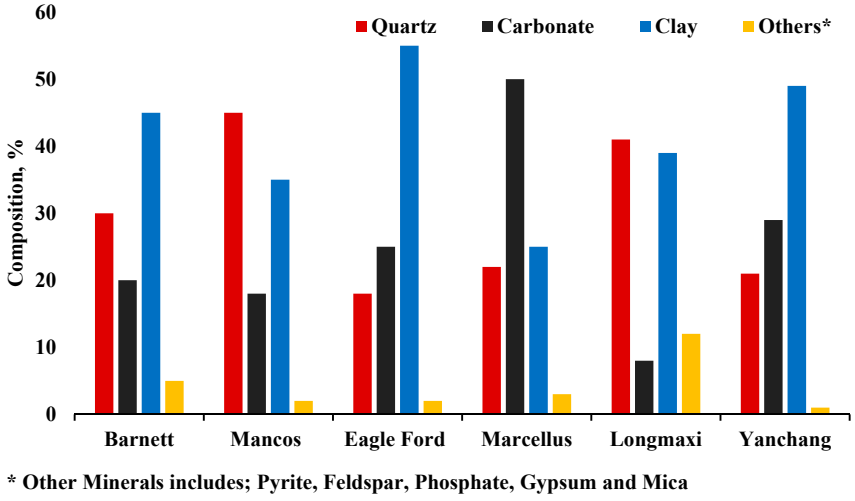

Figure 3. Typical mineral compositions of some shale formations.

Lahann et al. [56] addressed the mineralogical and petrophysical alteration of New Albany shales associated with the CO_2 injection, indicating that various alterations in Brunauer–Emmett–Teller (BET)-specific surface area of the mesopore and micropore structure system could occur. At high

pressure and temperature (24 MPa and 150 °C, respectively), the BET-SSA of both mesopore and micropore has increased with extended CO_2 injection treatment time, mainly because of the gradual increase in CO_2 solubility to dissolve carbonate minerals such as Ca^{++} and Mg^{++} at high pressures (Figures 4 and 5). A later study by Jiang et al. [55] has confirmed that $SCCO_2$ injection led to increasing SSA and porosity of Longmaxi shales with extending the treatment time, due to the extraction of organic matter from shale by $SCCO_2$, which can be related to the grain size of shale. Moreover, with increasing the pressure, the $SCCO_2$ density rises, permitting more organic matter to be dissolved in shale, thus increasing shale porosity [66–69]. Figure 6 shows the relationship between SSA and porosity at different $SCCO_2$ treatment pressures.

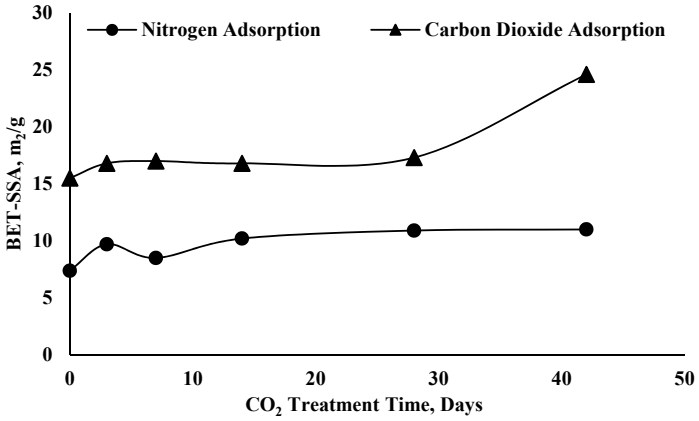

Figure 4. The effect of CO_2 treatment time on specific surface area (SSA) of New Albany shale at 150 °C [56].

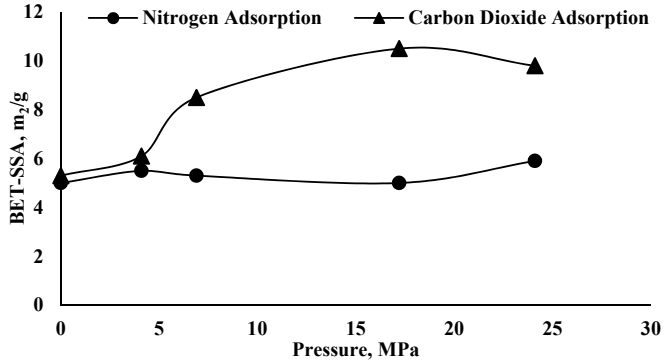

Figure 5. The effect of CO_2 treatment pressure on SSA of New Albany shale at 150 °C [56].

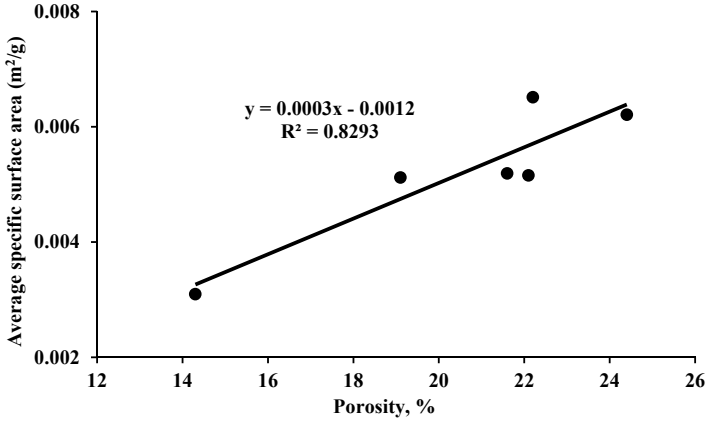

Figure 6. The relationship between SSA and porosity at different SC-CO_2 treatment pressures [55].

Recent studies [18,30,39,43,49–51] have further investigated the changes in the structural system of shales associated with $SCCO_2$ injection, and following points can be concluded: (1) the extraction of organic matter and the dissolution of carbonate minerals by $SCCO_2$ are the main causes for altering the pore structure system of shales, with a significant effect on micropores' and mesopores structure. (2) In the long-term, high pressure and temperature could result in more extraction of organic matter in shale, which in return reduces the CO_2 storage capacity. (3) The changes in shale's SSA and TPV are strongly related to the type of shale formation in term of surface mineralogy, surface morphology, and TOC; for instance, organic-rich shales are more likely to exhibit an increase in pore system [49,51,55,56], while the porosity and SSA of silty and low thermal maturity shales may decrease after $SCCO_2$ treatment [18,30,39,43].

The CO_2–shale interaction can also affect the shale's fractal dimensions after $SCCO_2$ exposure. Shales generally have complex inner porosity and irregular surface morphology, and the fractal dimension (D) index is used to quantitatively evaluate the structural complexity and surface roughness of solids [70]. Yin et al. [30] reported a reduction in the shale surface roughness caused by the CO_2 adsorption-induced swelling, which gradually transformed the surface morphology of shales from an irregular-complex structure to a smooth-regular structure. Consistently, Pan et al. [39] concluded that the extraction of organic matter in shales is the main mechanism for reducing the fractal dimensions of micropores structure after $SCCO_2$ treatment. However, a recent study by Luo et al. [50] reported opposite results, indicating an increase in the fractal dimensions and surface roughness of shale, which increases the complexity of the pore structure. This can be related to the dissolution of clay and carbonate minerals, which results in increasing the micropores' structure. This disagreement in results shows that the mineral genesis, mineral composition and sedimentary environment of shale could influence the fractal dimensions and surface roughness of shale.

In the long-term, the alteration in pore structure can affect the hydrocarbon transport during ESGR process, the sealing mechanism, and lead to lower CO_2 adsorption capacity [55]. The dynamic sealing efficiency of shales after $SCCO_2$ exposure was examined by Rezaee et al. [51], over time, a possible CO_2 leakage could occur due to the increase in pore volume, and the reduction in the capillary threshold pressure. This alteration in pore structure and capillary pressure is caused by the dissolution and precipitation of kaolinite, silica, and gypsum, which results in decreased CO_2 adsorption capacity, which is not favorable for CO_2 sequestration [18]. Alteration of pore structure during $SCCO_2$ injection could have a direct impact on other shale properties, including chemical and mechanical properties, as explained later in this paper. Therefore, it is crucial to examine the changes in shale pore structure associated with $SCCO_2$ injection. The related literature has addressed the significant impact of pore structure alteration on CO_2 storage capacity and hydrocarbon flow pattern during ESGR, however, a different type of shales will indicate various alterations on pore structure, thus each shale formation should be evaluated separately before CCS projects [11]. Table 1 summarizes several studies that highlighted the effect of CO_2 injection on pore structure system.

Table 1. Summary of recent studies highlighting the effect of CO_2 injection on pore structure.

Author(s)	Alteration % in Pore Structure Parameters	Name and Type of Shale Formation	Exposure Pressure, Temperature and Time	Main Findings
Lahann et al. [56]	SSA (49.05%)	New Albany (Organic-rich)	4–24 MPa 150 °C 3–42 Days	They concluded that at high pressures, CO_2 solubility in water increases due to the high dissolution of carbonate minerals. This is the main cause of increasing the SSA of the mesopore and micropore structure.

Table 1. *Cont.*

Author(s)	Alteration % in Pore Structure Parameters	Name and Type of Shale Formation	Exposure Pressure, Temperature and Time	Main Findings
Jiang et al. [55]	SSA (99.39%); Porosity (58.33%)	Longmaxi (silty/organic-rich)	8–18 MPa 40–90 °C 1–5 Days	This study showed that both shale porosity and SSA are increased with increasing $SCCO_2$ treatment time and pressure, due to the increase in $SCCO_2$ density and dissolving capability to extract organic matter in shale.
Yin et al. [30]	SSA (−60.52%); TPV (−28.25%); D (−4.18%); R_A (82.01%)	Longmaxi (organic/low thermal maturity)	16 MPa 40 °C 30 Days	In this study, a significant reduction in SSA, TPV and shale's fractal dimensions was observed after 30 days of $SCCO_2$ treatment, while the average pore size increased. This behavior is related to organic matter dissolution in micropores by $SCCO_2$.
Ao et al. [43]	SSA (−70.27%)	Longmaxi (organic)	15 MPa 35 °C 5–20 Days	The specific surface area of shale was reduced after $SCCO_2$ treatment. Shale deformation was caused by $SCCO_2$ adsorption and gas pressure, which further affects the strength of shales.
Rezaee et al. [51]	Porosity (4.0%); Capillary Pressure (−52.74)	Latrobe Group (mix of mudstone/organic-rich)	15.17 MPa 66 °C 60 Days	They reported that the increase in pore structure and the reduction in capillary threshold pressure could decrease the caprock seal efficiency, and cause a possible CO_2 leakage
Pan et al. [39]	For Longmaxi: SSA (−42.91%); D (−5.99%) For Yanchang: SSA (94.09%); D (2.37%)	Yanchang (mix of mudstone/organic-rich) and Longmaxi (organic-rich with low thermal maturity)	15 MPa 80 °C 10–30 Days	They studied the changes in shale surface morphology and CO_2 adsorption. They found that at high temperatures (80 °C), $SCCO_2$ can dissolve and extract organic matter on the surface. Leading to the formation of carbonic acid, which in return causes the alteration of SSA and pore volume in nanopores structure.
Hui et al. [18]	For Longmaxi: SSA (−52.05%); TPV (−10.34%) For Yanchang: SSA (23.99%); TPV (−16.67%)	Yanchang (mix of mudstone/organic-rich), Longmaxi (organic-rich) and Wufeng (organic-rich)	18 MPa 60 °C 10 Days	It was found that the high-pressure CO_2 adsorption resulted in a significant reduction in SSA, affecting the structural and geochemical properties of shale. After CO_2 treatment, the CO_2 adsorption capacity decreased which is not favorable for CO_2 sequestration.
Luo et al. [50]	SSA (115.1%); TPV (24.78%); D (4.43%)	Yanchang (mudstone)	10 MPa 50 °C 50 Days	This study confirms that CO_2–shale interactions have a strong influence on the micropores of shale, indicating an increase in SSA and pore volume. It was also found that fractal dimensions of shale have increased due to the dissolution of the clay and carbonate minerals.

2.2. Mineral Composition

Researchers initially explained the influence of mineralogical composition on the reactivity of shales during CO_2 injection. $SCCO_2$ has high diffusivity and acts as an organic solvent to extract some organic and inorganic minerals, which may lead to an increase in the porosity of shale [55,71]. Previous studies indicated that the alteration in shale mineralogy after $SCCO_2$ treatment is mainly caused by the geochemical reaction with the formation brine in the presence of carbonate minerals such as dolomite and calcite [18,30,39,43,51,72]. Alemu et al. [72] found that carbonate-rich shales have high reactivity to CO_2 compared to clay-rich shales, due to the dissolution of carbonate minerals and the formation of smectite, which results in a significant increase in calcite concentration. The diffusion of carbonic acid leads to a significant reduction in the pH [53,56,73], leading to changes in the mineral contents of shale through a series of chemical reactions and reversible reactions [43,74], mainly including:

$$CO_2 + H_2O \leftrightarrow H_2CO_3 \leftrightarrow H^+ + HCO_3^- \leftrightarrow 2H^+ + CO_3^{2-}$$

$$CaCO_3 + H^+ HCO_3^- \leftrightarrow Ca^{2+} + CO_2 + H_2O$$

$$MgCO_3 + H^+ HCO_3^- \leftrightarrow Mg^{2+} + CO_2 + H_2O$$

$$Al_2O_3 + H^+ HCO_3^- \leftrightarrow 2Al^{3+} + CO_2 + H_2O$$

Few scholars [30,55] have analyzed the surface microstructure of shale and indicated various changes in clay minerals such as kaolinite montmorillonite, illite, and anorthite after $SCCO_2$ treatment, caused by the extraction and dissolution of the in situ substance by $SCCO_2$. Non-clay minerals such as quartz, pyrite, and feldspar are most likely to exhibit a relative increase in content after $SCCO_2$ treatment because silicate minerals are rich in Ca^{+2}, Mg^{+2} and Al^{+3},and have high dissolving potential in acidified water during CO_2 injection, which leads to precipitation as carbonate solids [30,43]. This is favorable for mineral trapping mechanisms during long-term CO_2 storage. The phenomenon of mineral alteration in shales after $SCCO_2$ treatment was reported by the latest studies [18,39,49–51], indicating a high possibility for increasing quartz percentage and reduction in carbonate and clay minerals contents caused by CO_2-induced swelling, which affects CO_2 adsorption behavior.

During CO_2 injection, carbonic acid can also mobilize major and trace elements, affecting the physical structure of shales [75–77]. Recently, a study by Luo et al. [50] concluded that the hydrolysis and carbonation of silicate minerals is the main cause of element mobilization; minerals such as calcite, calcium, magnesium, sodium, potassium, and aluminum could face varying degrees of mobilization, which is controlled by the mineral composition and occurrence. However, it is important to consider the minerals' alteration for shale formation before CCS projects, as some elements with a high mobility such as zinc, cobalt, barium, and strontium may cause severe groundwater contamination [50]. The mineralogical alteration after $SCCO_2$ injection can cause major changes in the petro-physical properties of shales; as reported in the literature, the possible increase in micropore volumes might be beneficial for CCS and ESGR applications. Moreover, the long-term geochemical reactions provide a significant opportunity for mineralization trapping in shale formations, which plays an important role in increasing CO_2 storage capacity. However, further studies are required to capture the long-term mineral trapping mechanisms, especially mineral carbonation associated with CO_2 injection, and address the involved factors such as mineral type, pressure, and temperature [74].

2.3. Chemical Properties

Understanding the chemical reactions between CO_2, shales and formation water are very crucial for the practical application of CO_2 geological sequestration. The reactivity of shales to CO_2 depends mainly on the rock mineralogy, which eventually affects the chemical properties of the shale. Additionally, the fluid chemistry of CO_2 controls the dissolution and precipitation processes, and significantly impact the pore structure [72]. The alteration in shale chemical properties during CO_2 injection can be

understood by evaluating the surface chemistry of the shale and its functional groups' distribution through FTIR and *X*-ray photoelectron spectroscopy analysis [78]. Several studies [18,30,39,59,79] have reported that the presence of oxygen-containing groups on the shale surface such as −COOH, −H and −OH bonds, would have a severe impact for both CO_2 and CH_4 adsorptions on carbonate minerals at high pressures.

CO_2 injection causes a reduction in the intensity of C-O bonds in shales as well as aliphatic hydrocarbon (C-H) groups, which is related to the extraction of organic matter [39,71]. Yin et al. [30] suggested that some inorganic vibrational bands of quartz and illite (Si-O, Al-O-H and Si-O-Al bonds) can exhibit high absorption in shales similar to calcite and dolomite. Additionally, a noticeable reduction in aliphatic hydrocarbon groups was observed after CO_2 treatment, which confirms the associated changes in mineral contents. Recently, Pan et al. [39] proved that CO_2 injection can decrease the adsorption of the aliphatic hydrocarbon group, caused by the ability of CO_2 to dissolve the non-polar aliphatic and polar aromatic hydrocarbons. These alterations in hydroxyl functional groups (groups with oxygen) could increase CO_2 adsorption and affect the overall storage capacity.

Similarly, Hui et al. [18] confirmed that the chemical reactions between $SCCO_2$ and shales could decrease the oxygen-containing functional groups (C-O, O-C-O, C=O, COO−), and relatively increase the hydrogen groups (C-C/C-H) due to the ability of $SCCO_2$ to extract organics from the shale surface. This conclusion was based on the results obtained from three different shale formations after being treated with $SCCO_2$ as shown in Table 2. These relative alterations in oxygen and hydrogen functional groups can be explained by two points, (1) the evaporation and extraction behavior of $SCCO_2$ [18], and (2) the ability of $SCCO_2$ to extract organic matter and dissolve the polar kerogen moieties from shale surface [71,80]. As mentioned before, this alteration in surface chemistry and functional species after CO_2 injection could increase the CO_2 adsorption capacity in shales, thus more investigations are required to clarify the impact of chemical properties' alteration on the sequestration potential of CO_2 in shales.

Table 2. Changes in Hydrogen and Oxygen Functional Groups after $SCCO_2$ saturation [18].

Formation	Treatment Time, Hours	Hydrogen Functional Groups {C-C/C-H}, (%)	Increasing %	Oxygen Functional Groups {C-O, CO_3^{-2}, C=O, COO-}, (%)	Reduction %
Yanchang	0	74.11	6.06	25.89	17.34
	240	78.60		21.40	
Marine Longmaxi	0	57.41	11.18	42.59	15.07
	240	63.83		36.17	
Marine Wufeng	0	52.36	3.53	47.64	3.88
	240	54.21		45.79	

2.4. Surface Wettability

Shales' surface wettability is one of the major petro-physical properties that is affected by CO_2 injection. Wettability is defined as the affinity of the rock surface to a particular fluid; it is mainly affected by the rock surface mineralogy and temperature [81,82]. Understanding the wettability of shales is important as it controls the capillary forces, the relative permeability and hydrocarbon production [83]. Characterizing the wettability of shales can be challenging because of the nano-Darcy permeability, the porous medium heterogeneity and the presence of clay minerals with the variety of organic and inorganic matrix [84]. Hence, it is necessary to address the complex nature of shales' wettability and analyze the factors involved, i.e., pressure, temperature, pH, mineral composition and TOC [85]. Several studies were conducted to evaluate the wetting behavior of different types of shales at the presence of different fluids, by using different methods and techniques, such as equilibrium contact angle (sessile drop) [44,86–90], NMR [91], spontaneous imbibition [92–96], and liquid–liquid extraction [87].

Based on the related literature, it was reported that (1) shales usually have a mixed wettability, which can be related to the presence of organic matter [86], (2) the shale surface is originally hydrophilic at atmosphere pressure, due to the existence of clay minerals and other non-clay minerals such as quartz, feldspar, and dolomite in high fragments [60,83], and (3) the contact angle between CO_2 and shales increases with increasing pressure and temperature [44]. A recent review by Siddiqui et al. [85] claimed that under in situ conditions, the wettability system of hydrocarbon/brine/shale is preferentially water-wet, regardless of the mineral composition and type of hydrocarbon. The strong water-wetting behavior of shales in the presence of hydrocarbons works in favor of storage applications, as it increases the structural storage capacity. However, in the presence of CO_2, several studies suggested that pure minerals in the caprock are not entirely water-wet and highly influenced by the CO_2–rock interactions [42,45,46,97]. A high possibility of CO_2 migration may occur when shales become CO_2-wet; CO_2 could escape back into the atmosphere or the overlying aquifers [12]. This alteration in wettability will dramatically minimize CO_2 storage capacities, and reduce the sealing efficiency, which is the main sealing mechanism [12,47].

During the first decades of CO_2 storage, a possibility of CO_2 leakage may occur, when the capillary threshold pressure is reached; this may lower the structural trapping capacity and the overall efficiency of CO_2 sequestration [46,47,98]. Although shales display ultra-low permeability, they might still have a possibility of CO_2 breakthrough depending on the presented minerals [42,48]. It is important to highlight the primary trapping mechanisms for CO_2 sequestration in shales, which are: (1) structural trapping, where shale formations act as a caprock [65,99]; (2) residual trapping, where capillary forces restrict the movement of CO_2 in the shale pores [100,101]. However, during ESGR processes, mineral trapping may also occur in some shale formations, due to the interactions between CO_2 and shale mineralogy; this mineral dissolution allows the CO_2 to enter the reservoir interlayers, and increases the CO_2 storage capacity [40,47].

In the last decade, several scholars have investigated the factors affecting the CO_2 wettability behavior of caprocks [12,45–47,52,98,102–104]. Mineral composition and surface chemistry were found to have significant influences on the structural trapping capacity, besides other factors including organic matter, brine salinity, pressure and temperature. Iglauer et al. [46] found that CO_2 wettability of caprock increases with increasing pressure, indicating a poor water-wet or intermediate-wet, which may affect the sealing efficiency. Chaudhary et al. [103] also reported a high contact angle between CO_2 and shale at 22.8 MPa, indicating a mixed-wet behavior. On the contrary, low contact angles between CO_2 and silty shales were reported by Kaveh et al. [45], which indicate a strong hydrophilic caprock system even at high pressures. When the contact angles between CO_2 and shale are low, CO_2 becomes immobilized by the high capillary forces in the pore structure of the shale. However, increasing the contact angles decreases the capillary force and allows CO_2 to move upward by the buoyancy forces, and thus increases the chances of capillary breakthrough. Surface wettability is mainly affected by the shale's mineralogical composition, therefore different wetting behaviors could occur for different shale geometries [47]. Factors including brine salinity, temperature, organic content and thermal maturity, were found to have minor impacts on CO_2/shale contact angles. Strong water-wet behavior was observed in several studies despite the high concentrations of organic content, brine salinities and thermal maturities [12,45].

The injection of CO_2 into shales was also found to increase the contact angle between brine and shales, and reduce the shale surface hydrophilicity [52]. This can be related to the release of water content from clay minerals during CO_2 treatment. Moreover, the increase in shale-water contact angles causes a relative reduction in the surface tension between shale and water. This can be attributed to the adsorption capacity of solid surfaces and the CO_2 diffusion into the shale matrix after CO_2 treatment. Figure 7 shows the relationship between the $SCCO_2$ treatment time and pressure on the shale–water contact angle. Accurate characterization of CO_2 wettability of shales is useful to estimate CO_2 storage capacity, and essential to determine the technical feasibility for CO_2 sequestration and hydrocarbon flow dynamics during the ESGR process [22]. Despite the progress achieved in the related literature on

CO_2 wetting in shales, the knowledge on wettability alteration is still evolving, and more insights are required to answer some decisive questions, i.e., what is the wetting behavior of different shales at various length scales? What mineral composition will prevent CO_2 capillary leakage [12]?

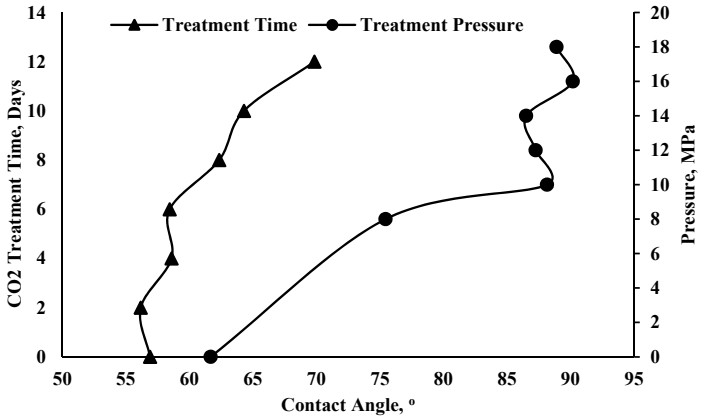

Figure 7. The changes in contact angle associated with $SCCO_2$ treatment time and pressure [52].

Table 3 highlights the related work on the changes in shales' contact angles values associated with CO_2 injection at different operating parameters, and the subsequent impact on shales' wettability.

Table 3. Summary of related work on the effect of CO_2 injection on wettability and contact angle.

Author(s)	Wettability System	Contact Angle Measurement Method	Pressure and Temperature	Main Findings	Effect on Storage Capacity and CO_2 Leakage Possibility
Chiquet et al. [42]	CO_2/Brine/ (Mica-Quartz)	Contact angle (captive-drop)	3.5–11 MPa Unknown temperature	Contact angle measurements were conducted on shaly caprock minerals (mica and quartz), indicating that the presence of CO_2 significantly increases the contact angle. This behavior altered the wettability from water-wet to intermediate-wet at high pressures, caused by the CO_2 dissolution and brine pH reduction.	Decreasing in CO_2 storage capacity. CO_2 leaks more easily due to the increase in contact angles and IFTs.
Zhu et al. [83]	CO_2/Brine/Rock	Contact angle (Wilhelm plate method)	Atmospheric pressure 50, 70 °C	This study indicated that tight rocks' wettability can be altered after CO_2–brine–shale interactions, due to the dissolution and precipitation of the minerals. The contact angles increases after the CO_2 injection with increasing CO_2 treatment pressure at 50 °C.	Continuous dissolution of carbonate minerals may increase the percentage of some elements (O and Si) on the shale surface, which reduces the possibility of CO_2 leakage.
Iglauer et al. [46]	CO_2/Brine/Rock	Tilted plate method	10–20 MPa 50 °C	In this study, the CO_2 wettability of several natural caprock samples was tested at various pressures. They found that CO_2 wettability of caprock increased at high pressure of 20Mpa, indicating an intermediate-wet to poor-wet behavior.	Noticeable reduction in the sealing efficiency implies possible CO_2 leakage. Structural trapping capacity is reduced significantly.

Table 3. *Cont.*

Author(s)	Wettability System	Contact Angle Measurement Method	Pressure and Temperature	Main Findings	Effect on Storage Capacity and CO_2 Leakage Possibility
Chaudhary et al. [103]	CO_2/brine/ Organic Shale	High-resolution X-ray computed tomography (HRXCT)	13.8–22.8 MPa 60–71 °C	In this study, the authors presented a new method to measure the contact angle and wettability behavior of minerals at reservoir conditions. This method is based on the usage of X-ray imaging and radiography. They reported an increase in the contact angle at a pressure of 22.8 MPa. This confirms the ability of CO_2 to alter minerals wettability due to dissolution behavior.	The contact angle in organic-rich shale increased to (59°). However, the shale surface indicated a water-wet behavior. This implies stronger storage capacity and low leakage potential.
Kaveh et al. [45]	CO_2/water/Silty Shale	Contact angle (pendant-drop)	0.2–15 MPa 45 °C	They examined the wettability of silty shale with CO_2 and water under various temperatures and pressures. The results showed that the silty shale remains hydrophilic at high pressures. They also found that the wettability system slightly increases with decreasing temperature.	Silty shales show strong water-wet behavior, indicating a low possibility of CO_2 capillary breakthrough, and high storage capacity.
Guiltinan et al. [12]	brine/CO_2/ organic-rich shale	X-ray computer tomography scanning	13.79 MPa 20,40,60 °C	This study investigated the effect of organic matter and thermal maturity on the CO_2 wettability of shales. The results showed that the wettability system remains strong water-wet despite the changes in concentrations of organic content and thermal maturities.	This behavior has no major influence on the efficiency of structural trapping (low leakage potential) and is favorable for CO_2 sequestration.
Qin et al. [52]	Water/shale contact angles	Contact angle (pendant-drop)	Atmospheric pressure 25 °C	In this study, treatment time and pressure led to a significant increase the contact angles, due to the decrease in carbonate mineral content and the release of water content from clay minerals during the treatment.	The hydrophilicity of the shale surface decreases, which may result in CO_2 leakage and lower capacity.

2.5. Mechanical Properties

The dissolution and precipitation of minerals after CO_2 injection causes significant alterations in the mechanical properties of shales, which raises stability concerns for the long-term CO_2 sequestration. Generally, the changes in pore structure and mineral content caused by CO_2 injection reflect the possible deformation and weakening in the strength of caprocks, and thus reduces the overall CO_2 adsorption capacity [74]. Several studies were conducted to investigate the effect of CO_2 injection on rocks' mechanical properties, and evaluate the associated factors including treatment time, pressure, CO_2 phase state, and bedding angles [27,41,74,105]. The injection of acid gases such as CO_2 and H_2S together with carbonated water was found to alter the physical properties of chalk, and affect the displacement behavior under in situ conditions, which eventually reduced the chalk strength and ductility [106,107]. Similarly, deformation in sandstone and siltstone formations was observed after the injection of $SCCO_2$ [108], which led to increasing the porosity and precipitation of calcite [109,110]. This deformation behavior in caprock can be attributed to the changes in effective stress and crack propagation, which increases the potential of CO_2 leakage.

The alteration of coal mechanical properties is affected by pressure and CO_2 phase state [111–115]. Coal seams are significantly weakened by the injection of $SCCO_2$ compared to gaseous and Sub-critical CO_2. Viete and Ranjith reported a reduction of 13% and 26% in both compressive strength and elastic modulus, respectively, after $SCCO_2$ injection [112]. Such an effect is caused by the high $SCCO_2$ adsorption in coals and the permeability increase under in situ conditions. Shale formations have a strong ability to adsorb CO_2, and such behavior causes a reduction in effective stress, increasing the compression and raising the pore pressure within the formation [43,116]. This results in shale swelling, decreasing strength and brittleness, and eventually damaging the shale formations. Few recent scholars have investigated the effect of different factors on shale mechanical properties after CO_2 injection [27,41,43,49,74,105]. The analysis of uniaxial compressive strength (UCS) and Young's modulus (E), are commonly used to evaluate the stress conditions of shales through conducting uniaxial and triaxial compression tests [117].

Increasing the CO_2 treatment time of black shale was found to reduce both UCS and E values drastically by 66.05% and 56.32%, respectively, after 30 days [74]. This also results in decreasing the shale's brittleness index, and increasing its plasticity and toughness. When CO_2 interacts with black shale, carbonate minerals precipitate as calcite and cause a reduction in the stress in the formation. Besides, the dissolution of clay minerals exhibits possible damage in shale macroscopic structure, which, as a result, increases the initial compaction and reduces shale strength [49]. CO_2 phases and saturation pressure were also found to affect shale mechanical properties. Saturating organic-rich shales with $SCCO_2$ for 10 days reduced UCS and E by 22.86% and 23.10%, respectively [41]. $SCCO_2$ has a stronger ability to increase the crack initiation pressure compared to gaseous CO_2, and thus reduce the crack damage stress. This results in shale swelling and creating more micro-cracks within the shale formation, and subsequently reduces the strength [27,41]. Moreover, increasing saturation pressure beyond 12 MPa showed a minor impact on reducing UCS and E due to the compression effect of fluid [49]. The mechanical properties of shales could also be influenced by the bedding orientation and the various forces generated, i.e., normal, shear, and compressive stresses along the bedding plane [105]. The direction of normal and shear stresses is dependent on the bedding angle, which results in differences in the degree of deformation in shale. At a bedding angle of 0°, only normal stress exists, which promotes the development of tensile failure [105]. In such a case, the cracks deviate through the damaged bedding direction which causes shale weakening. However, increasing the bedding angle beyond 45° sustains the shale strength and the resistance to crack propagation, which is related to the development of both tensile and shear failures.

The weakening of shales was further clarified by later studies [27,43,49,105], which reported various reductions in mechanical strength after $SCCO_2$ injection, due to the dissolution effect and adsorption strain within the pores. It should be highlighted that the resulted physical changes in shales after CO_2 injection, were found to have a significant impact on the shale strength [49]. The associated reduction in mesopores volume can partially destroy the shale skeleton density and weakens the shale. Based on the related literature, it is apparent that CO_2-shale interaction may significantly reduce the mechanical parameters and weaken strength and brittleness of the shales. This degradation in shale mechanical properties is caused by several factors, which require further assessment in the future. Because of the heterogeneity of shale, it is essential to characterize each shale formation on a case-by-case basis to ensure the stability of shale formations during CCS.

Table 4 summarizes recent studies that highlighted the effect of CO_2 injection on mechanical properties.

Table 4. Summary of recent studies highlighting the effect of CO_2 injection on mechanical properties.

Author(s)	Reduction % in Measured Parameters	Name and Type of Shale Formation	Exposure Pressure, Temperature and Time	Main Findings
Lyu et al. [74]	UCS (66.05%); *E* (56.32%); BI (50%)	Longmaxi (Black shale)	9 MPa 40 °C 10–30 Days	This study evaluated the effect of different $SCCO_2$ saturation time on UCS and Young's modulus of black shales. They observed a clear reduction in shale strength and brittleness index, after 10 days of saturation, due to the dissolution of clay minerals, with more reduction after 30 days.
Ao et al. [43]	Tensile Strength (22.7%); Tri-axial compressive strength (15.3%); *E* (29.56%)	Longmaxi (organic)	15 MPa 35 °C 5–20 Days	They reported a gradual reduction in tensile strength and triaxial compressive strength of the shales with increasing $SCCO_2$ treatment time.
Yin et al. [41]	UCS (22.86%); *E* (23.10%)	Longmaxi (organic-rich)	4–16 MPa 38 °C 10 Days	This study reported the impact of saturation pressure and CO_2 phase on shale mechanical properties. The results showed that $SSCO_2$ has more influence on UCS and E than $subCO_2$, due to the high adsorption and dissolution capacity for $SCCO_2$. Consistently, a noticeable increase was observed in the Crack initiation pressure and a reduction in crack damage stress, which indicates the creation of more micro-cracks by $SCCO_2$.
Lyu et al. [27]	UCS (30%); *E* (38%)	Sichuan Basin (low-clay)	9 MPa 40 °C 10–30 Days	The ability of CO_2 adsorption in weakening the shale strength and increasing its ductility was addressed. A clear reduction in UCS and E was found on the $SCCO_2$ treated shale samples, with a noticeable increase in crack initiation and the decrease in crack damage.
Feng et al. [105]	Brazilian splitting strength (BSS) (46%); Absorbed energy (U) (50%); *E* (22%)	Sichuan Basin (Black shale)	10 MPa 40 °C 10–60 Days	This study investigated the effect of $SCCO_2$ saturation time and bedding orientation on shale strength. They concluded that the damage caused by $SCCO_2$ in the pore structure is the key cause of mechanical degradation. Noticeable changes were observed in shale strength with changing the bedding angles (θ); both tensile and shear failure could occur affecting the shale resistance and cracking propagation.
Lu et al. [49]	UCS (31%); *E* (10%)	Yanchang (mudstone)	12 MPa 50 °C 8 Days	This study found a strong connection between the damage in pore structure and the weakening of shale strength. The possible damage in shale macroscopic structure increases the stress–strain in the initial compaction stage, which results in reducing shale strength.

3. Environmental Evaluation of CCS

The environmental consequences of CCS are often evaluated through Life Cycle Assessment (LCA) studies. LCA is proven to provide a complete analysis of all environmental effects of applying CCS to power plants. Such studies are detailed and time-consuming and vary in scope, methodology and outcomes, but they provide a suitable assessment of many environmental effects, including global warming potential (GWP), acidification potential (AP), eutrophication potential (EP), photochemical

ozone creation potential (POCP) and cumulative energy demand (CED) [118]. Several studies have performed LCA on different CCS power plants [119–123], and the majority of these studies indicated a clear reduction in GWP, regardless of the technology used in transport, injection and storage of CO_2 [118]. Generally, there are three main factors incorporated to influence the environmental effects from the CCS systems [124]: (1) efficiency energy penalty, (2) purity and capture efficiency of CO_2, and (3) origin and composition of the fuel. However, CO_2 capturing is out of the scope of the current study.

Energy penalties are associated with the capture technology, generally, pre-combustion processes produce lower energy penalties compared to pre-combustion and oxyfuel processes [119,120]. For instance, 29.6% of post-combustion thermal efficiency for hard coal was reported by Schreiber et al. [122], while 48% thermal efficiency was reported with pre-combustion process [120]. This variation can be attributed to the different types of fuel composition (natural gas, coal), assumptions in time scale, and the different energy sources (gas, hard coal, bituminous, lignite) [124]. For an electricity production process, CO_2 is produced in different purities and captured by the different systems. Therefore by minimizing the consumption of electricity for the CO_2 capture, the energy penalty is reduced, and thus reduces the environmental effects from the CCS system [124]. Hard coal is considered as a valuable and wide available fuel to capture CO_2; one LCA study shows that the power generation from hard coal has significantly reduced the GWP, indicating about 13% contribution to the total GWP for post-combustion [123]. Similarly, the power generation from lignite power plant reduces the GWP, with lower share to the global total GWP compared to hard coal [121], due to the production of mono-ethanolamine during the capture process. However, natural gas implies higher efficiency in capturing process compared to hard coal and lignite, with a reported thermal efficiency of 49.6% and 44.7% in post-combustion and oxyfuel processes, respectively [122]. This results in lowering the GWP of power plants and increases the efficiency in CO_2 capture.

Other environmental effects including AP, EP, POCP and CED showed inconsistent results for different energy power plants and capture technology [124]. For instance, post-combustion hard coal power generation systems indicated an increase in the EP compared with the power plants without CCS [124], while a 15% reduction in EP was reported at the lignite oxyfuel system [121]. This inconsistency between hard coal and lignite can be related to the capture technology used (post-combustion and oxyfuel, respectively), and long transport distance required in hard coal systems [124]. However, for natural gas systems, the EP usually increases, as it is mainly dominated by emissions from operation regardless of the capture technology [118]. An increase in EP by 266–403% was reported for natural gas systems when using a steam integrated system for CO_2 delivery [118]. Similarly, a range between a 15% and 50% increase in EP was reported in several studies [119,121–123]. Therefore, no solid conclusion can be made regarding the assessment of EP and other environmental effects, due to the lack of sufficient data in the literature. In LCA studies, the selection of the time scale is crucial for reliable evaluation. Considering the present and future power plants for extended duration allows us to predict the main production processes and consider future modification [120,125]. Moreover, sensitivity analysis on the time scale could help to assess the storage process and identifying possible leakage [119,121]. However, it is not clear how possible storage leakage will impact the environmental effects, as it is difficult to perform climate conditions forecasts. Other factors are considered in LCAs, including compression, pipeline transport, injection and storage of CO_2 indicate almost negligible impacts for all environmental effects [118].

In summary, LCA studies vary in the technologies used for the CO_2 capture and storage, and the existing literature is too scarce to draw a solid conclusion. However, LCA still provides an idea of the impact of CCS on environmental performance, and a general understanding of the influence of capture efficiency, energy penalty and fuel composition. In future LCA studies, several aspects shall be considered, including techniques for CO_2 capture, modeling leakage potential and incorporating both conventional and renewable energy resources [124].

4. Economic Viability of CCS in Shales

Shale formations hold a promising potential to utilize CCS projects in terms of their technical feasibility. By combining ESGR operations with long-term CO_2 storage applications, CH_4 production can be maximized due to the strong adsorption capacity of CO_2. However, the economic viability of CCS in shales has yet to be proven, as the related literature on this topic is limited. Considering the associated costs of CO_2 capture, transport, and storage, together with infrastructure cost and petro-physical characteristics of shales could make CCS project costly [126,127]. Therefore, in this paper, we briefly highlight the main challenges facing the economic viability of CCS in shales. The costs of CO_2 capture were studied and analyzed earlier in the 21st century, and enormous reports were presented based on the plant type (source) and capture technique (Table 5). Mainly, there are two components of the cost of CO_2 capture. First is the cost of removing CO_2 from industrial emissions, as, currently, chemical adsorption of CO_2 is believed to be the best available technology [128]. Secondly, the cost of equipment and chemicals, as they increase the overall capture capital cost. CO_2 capture is more of a technical factor, and innovative technologies are needed to reduce the costs of CO_2 capture and deliver stable long-term benefits [34].

The costs of CO_2 injection and transportation are dominant factors affecting the economic viability of CCS in shales. These costs are controlled by the potential revenue form CH_4 production and other factors including well spacing, CO_2 separation, and bottom-hole pressure [129]. The CO_2 injection cost is related directly to the CO_2 injectivity approach used, i.e., the applied huff-n-puff processes in the Big Sinking Field showed an increase in injection cost by USD 0.35/metric tonnes [130]. Although CO_2 injection is costly, integrated CCS systems in shales estimated a reduction of 30% on the average of the CO_2 injection cost, with an average of USD 5–10/metric tonnes lower cost compared to saline aquifer [131]. The main reasons behind this are as follows: one is the gradual reduction in pore pressure during CO_2 injection in shales and the production of CH_4; two is the large storage potential for shales.

However, the added cost of CO_2 transportation is large compared to injection and capture costs. A study [129] on Marcellus shales estimated a cost of USD 60–70/metric tonnes to transport CO_2 from industrial source to the site, added to the USD 22.4/metric cost of for CO_2 injection. These results indicate that using shorter pipeline transport distances with smaller diameters could be a suitable method to reduce the transport cost, which eventually implies high incremental capital costs. Moreover, utilizing high bottom-hole pressure wells with a short distance between producer and injector wells could reduce the total cost of CCS to USD 39/metric tonnes and provide more storage potential due to high injection pressure. The cost of infrastructure—which includes CO_2 storage hubs and pipelines—is less costly compared to CO_2 injection, transport and capture, nevertheless, they should be carefully assessed and included in economic viability studies.

Apart from the consideration of the fixed costs, the application of CCS is derived by other factors, mainly related to the concerns regarding carbon price and carbon tax revenues [132]. Addressing this topic is within the gaps between the economic theory and reality that prevents CCS to have an international breakthrough [133]. Another concern about integrated CCS systems is how they can be utilized for large-scale fossil fuel power plants instead of refining industries only. However, reviewing and discussing these factors is out of the scope of this paper, yet it is reliable for generally highlighting these economic drivers and their impact on CCS deployment (Table 6). In summary, more studies are needed to provide clear assessments of economic viability of CCS in shales. Although the application of CCS in shales is encouraging, the lack of available knowledge regarding storage capacity, reservoir data for best sequestration settings and the effect of long-term CO_2/shale interaction can affect its economic viability.

Table 5. Early studies on estimated CO_2 capture cost from different plants [129].

Author(s)	CO_2 Capture Cost, $/Metric Tonnes	Plant Type (Source)
Smith et al. [134]	21–62	Coal-based Integrated gasification combined cycle (IGCC)
Heddle et al. [135]	14.55	N/A
Rubin et al. [136]	29–44	Pulverized coal combustion (PC)
	11–32	Coal-based Integrated gasification combined cycle (IGCC)
	28–57	Natural gas combined cycle (NGCC)
Holloway [137]	18–72	Power Plant
Finkenrath [138]	43–62	N/A

Table 6. Economic drivers for CCS projects [133].

Environmental Policy	Cost of CCS	Fossil Fuel Energy Costs	Clean Energy Sources
This is the main driver for CCS technology, as it controls the economic market and energy generation. The demand for CCS will depend on the employed strategy that targets carbon emissions through "carbon tax" revenues. When carbon emissions are optimally taxed, this allows for the non-energy cost of CCS to drop, and thus lowers the emissions tax [132]. In this case, a lower carbon tax provides the opportunity for companies to apply CCS projects.	For the CCS project to be cost-effective, the unit cost to capture, transport and storage has to be lower than the emitting CO_2 and pay the carbon price. A more advanced CCS technology will lead to an increase in energy generation from fossil fuels and reduce the unit cost of CCS. Moreover, the availability of geological sequestration sites will also result in a higher level of CCS.	Fossil fuel resources are limited in nature, and the increase of generating fossil fuel energy costs will affect the level of fossil fuel energy, carbon emissions, and overall CCS activity. Therefore, due to the exhaustibility and scarcity rent cost, renewable resources should be considered as a possible alternative for fossil fuels, which may help to achieve a higher level of CCS [139].	There is an approach to utilize carbon-free resources i.e., solar energy, wind and nuclear electric power to replace or at least contribute to energy generated from fossil fuels. It will be ideal to employ clean energy sources only, as generating energy cost is low, which puts CCS in high demand, but the full replacement of fossil fuels is not expected soon. As of today, 80% of the global energy needs are supplied by fossil fuels, however, by combining both sources with optimal timing, the cost of energy generation can be reduced, and thus increases the level of CCS [140].

5. Conclusions

CO_2/shale interaction is a significant factor for the efficiency and the success of CCS technology in depleted shale formations, for its noticeable impact on altering shale physical, chemical, and mechanical properties. This paper presented the current knowledge of CO_2/shale interactions and provided a comprehensive review of the impact of CO_2 exposure on shale properties and the subsequent implications on CO_2 storage. The accomplishments achieved through laboratory experiments confirm that the physical structure and surface chemistry of shales are highly influenced by CO_2 injection, due to the formation of carbonic acid within shales, which, in the long-term, might reduce CO_2 adsorption capacity and storage potential. Shale-sealing efficiency is also affected by the injection of CO_2, as the presented minerals on the shale surface could decrease the shale surface hydrophilicity. Furthermore, CO_2 injection causes a massive degradation in shale mechanical properties, and a noticeable reduction in shale brittleness and increases in its plasticity and toughness were observed, which results in shale weakening. The knowledge of CO_2/shale interaction and its implications on CCS requires further study;

systematic studies are in need to evaluate the feasibility of CCS in shales technically and commercially. With this evolving technology comes many technical and economical unknowns, which shall be addressed in future work.

Author Contributions: In this review paper, A.F. wrote the draft paper with support from Z.B. on the paper structure and organization. H.B.M. and R.G. contributed with their valuable suggestions on the overall quality of the manuscript and also on other parts including the introduction, chemical properties and CCS viability sections. M.M.H. submitted the manuscript as a corresponding author and assisted with other authors in revising the manuscript according to reviewers' comments. All authors have read and agreed to the published version of the manuscript.

Funding: This research received no external funding.

Acknowledgments: The authors gratefully acknowledge Curtin University for providing financial support through the Curtin Malaysia Graduate School and Research and Development Office.

Conflicts of Interest: The authors declare no conflict of interest.

References

1. Metz, B.; Davidson, O.; de Coninck, H.; Loos, M.; Meyer, L. *Carbon Dioxide Capture and Storage*; Cambridge Univ. Press: New York, NY, USA, 2005.
2. de Silva, P.N.K.; Ranjith, P.G.; Choi, S.K. A study of methodologies for CO_2 storage capacity estimation of coal. *Fuel* **2012**, *91*, 1–15. [CrossRef]
3. Blunt, M.; Fayers, F.J.; Orr, F.M. Carbon dioxide in enhanced oil recovery. *Energy Convers. Manag.* **1993**, *34*, 1197–1204. [CrossRef]
4. Lackner, K.S. A guide to CO_2 sequestration. *Science* **2003**, *300*, 1677–1678. [CrossRef]
5. Holloway, S. An overview of the underground disposal of carbon dioxide. *Energy Convers. Manag.* **1997**, *38*, 193–198. [CrossRef]
6. Tao, Z.; Clarens, A. Estimating the carbon sequestration capacity of shale formations using methane production rates. *Environ. Sci. Technol.* **2013**, *47*, 11318–11325. [CrossRef]
7. Kang, S.M.; Fathi, E.; Ambrose, R.J.; Akkutlu, I.Y.; Sigal, R.F. Carbon dioxide storage capacity of organic-rich shales. *SPE J.* **2011**, *16*, 842–855. [CrossRef]
8. Perera, M.S.A. Influences of CO_2 Injection into Deep Coal Seams: A Review. *Energy Fuels* **2017**, *31*, 10324–10334. [CrossRef]
9. Merey, S.; Sinayuc, C. Analysis of carbon dioxide sequestration in shale gas reservoirs by using experimental adsorption data and adsorption models. *J. Nat. Gas Sci. Eng.* **2016**, *36*, 1087–1105. [CrossRef]
10. Liu, D.; Li, Y.; Agarwal, R.K. Numerical simulation of long-term storage of CO_2 in Yanchang shale reservoir of the Ordos basin in China. *Chem. Geol.* **2016**, *440*, 288–305. [CrossRef]
11. Zhou, J.; Hu, N.; Xian, X.; Zhou, L.; Tang, J.; Kang, Y.; Wang, H. Supercritical CO_2 fracking for enhanced shale gas recovery and CO_2 sequestration: Results, status and future challenges. *Adv. Geo-Energy Res.* **2019**, *3*, 207–224. [CrossRef]
12. Guiltinan, E.J.; Cardenas, M.B.; Bennett, P.C.; Zhang, T.; Espinoza, D.N. The effect of organic matter and thermal maturity on the wettability of supercritical CO_2 on organic shales. *Int. J. Greenh. Gas Control* **2017**, *65*, 15–22. [CrossRef]
13. Zhan, J.; Soo, E.; Fogwill, A.; Cheng, S.; Cai, H.; Zhang, K.; Chen, Z. A systematic reservoir simulation study on assessing the feasibility of CO_2 sequestration in shale gas reservoirs with potential enhanced gas recovery. *Carbon Manag. Technol. Conf. C 2017 Glob. CCUS Innov. Nexus* **2017**, *1*, 33–44.
14. Hoffman, A.; Gustaf, O.; Andreas, L. *Shale Gas and Hydraulic Fracturing: Framing the Water Issue*; Ineko: Stockholm, Sweden, 2014; Volume 34.
15. Nuttall, B.; Eble, C.; Drahovzal, J.; Bustin, R. *Analysis of Devonian Black Shales in Kentucky for Potential Carbon Dioxide Sequestration and Enhanced Natural*; Kentucky Geol. Surv.: Lexington, KY, USA, 2005.
16. Li, X.; Feng, Z.; Han, G.; Elsworth, D.; Marone, C.; Saffer, D. Hydraulic Fracturing in Shale with H_2O, CO_2 and N_2. In *49th US Rock Mechanics/Geomechanics Symposium*; American Rock Mechanics Association: San Francisco, CA, USA, 2015; pp. 1–8.
17. Zhenyun, S.; Weidong, S.; Yanzeng, Y.; Yong, L.; Zhihang, L.; Xiaoyu, W.; Li, Q.; Zhang, D.; Wang, Y. An experimental study on the CO_2/sand dry-frac process. *Nat. Gas Ind. B* **2015**, *1*, 192–196. [CrossRef]

18. Hui, D.; Pan, Y.; Luo, P.; Zhang, Y.; Sun, L.; Lin, C. Effect of supercritical CO_2 exposure on the high-pressure CO_2 adsorption performance of shales. *Fuel* **2019**, *247*, 57–66. [CrossRef]
19. EIA. *Outlook for Shale gas and Tight Oil Development in the U.S.*; Energy Information Administration: Washington, DC, USA, 2013.
20. King, G.E. Thirty Years of Gas Shale Fracturing: What Have We Learned? In *SPE Annual Technical Conference and Exhibition*; Society of Petroleum Engineers: Florence, Italy, 2010.
21. Wang, L.; Torres, A.; Xiang, L.; Fei, X.; Naido, A.; Wu, W. A Technical Review on Shale Gas Production and Unconventional Reservoirs Modeling. *Nat. Resour.* **2015**, *06*, 141–151. [CrossRef]
22. Middleton, R.S.; Carey, J.W.; Currier, R.P.; Hyman, J.D.; Kang, Q.; Karra, S.; Jiménez-Martínez, J.; Porter, M.L.; Viswanathan, H.S. Shale gas and non-aqueous fracturing fluids: Opportunities and challenges for supercritical CO_2. *Appl. Energy* **2015**, *147*, 500–509. [CrossRef]
23. Vesovic, V.; Wakeham, W.; Olchowy, G.; Sengers, J.; Watson, J.; Millat, J. The transport properties of carbon dioxide. *J. Phys. Chem.* **1990**, *19*, 763–808. [CrossRef]
24. Vermylen, J.P. Geomechanical Studies of the Barnett Shale. Ph.D Thesis, Stanford University, Stanford, CA, USA, 2011.
25. Jin, Z.; Firoozabadi, A. Effect of water on methane and carbon dioxide sorption in clay minerals by Monte Carlo simulations. *Fluid Phase Equilib.* **2014**, *382*, 10–20. [CrossRef]
26. Godec, M.; Koperna, G.; Petrusak, R.; Oudinot, A. Potential for enhanced gas recovery and CO_2 storage in the Marcellus Shale in the Eastern United States. *Int. J. Coal Geol.* **2013**, *118*, 95–104. [CrossRef]
27. Lyu, Q.; Long, X.; Ranjith, P.G.; Tan, J.; Kang, Y.; Wang, Z. Experimental investigation on the mechanical properties of a low-clay shale with different adsorption times in sub-/super-critical CO_2. *Energy* **2018**, *147*, 1288–1298. [CrossRef]
28. Liu, F.; Ellett, K.; Xiao, Y.; Rupp, J.A. Assessing the feasibility of CO_2 storage in the New Albany Shale (Devonian-Mississippian) with potential enhanced gas recovery using reservoir simulation. *Int. J. Greenh. Gas Control* **2013**, *17*, 111–126. [CrossRef]
29. Heller, R.; Zoback, M. Adsorption of methane and carbon dioxide on gas shale and pure mineral samples. *J. Unconv. Oil Gas Resour.* **2014**, *8*, 14–24. [CrossRef]
30. Yin, H.; Zhou, J.; Jiang, Y.; Xian, X.; Liu, Q. Physical and structural changes in shale associated with supercritical CO_2 exposure. *Fuel* **2016**, *184*, 289–303. [CrossRef]
31. Luo, X.; Wang, S.; Wang, Z.; Jing, Z.; Lv, M.; Zhai, Z.; Han, T. Adsorption of methane, carbon dioxide and their binary mixtures on Jurassic shale from the Qaidam Basin in China. *Int. J. Coal Geol.* **2015**, *150*, 210–223. [CrossRef]
32. Edwards, R.W.J.; Celia, M.A.; Bandilla, K.W.; Doster, F.; Kanno, C.M. A Model To Estimate Carbon Dioxide Injectivity and Storage Capacity for Geological Sequestration in Shale Gas Wells. *Environ. Sci. Technol.* **2015**, *49*, 9222–9229. [CrossRef]
33. Levine, J.S.; Fukai, I.; Soeder, D.J.; Bromhal, G.; Dilmore, R.M.; Guthrie, G.D.; Rodosta, T.; Sanguinito, S.; Frailey, S.; Gorecki, C.; et al. U.S. DOE NETL methodology for estimating the prospective CO_2 storage resource of shales at the national and regional scale. *Int. J. Greenh. Gas Control* **2016**, *51*, 81–94. [CrossRef]
34. Global CCS Institute, The Global Status os CCS 2018. Australia. 2018. Available online: https://www.globalccsinstitute.com (accessed on 26 March 2020).
35. Wang, T.U.S. Shale Gas and Tight Oil Plays Production 1999–2050. 2020. Available online: https://www.statista.com/statistics/183740/shale-gas-production-in-the-united-states-since-1999/ (accessed on 7 June 2020).
36. Wang, T. Forecast of Carbon Dioxide Emissions Worldwide from 2018 to 2050. 2019. Available online: https://www.statista.com/statistics/263980/forecast-of-global-carbon-dioxide-emissions/ (accessed on 7 June 2020).
37. Andrews, R. Global CO_2 Emissions Forecast to 2100. 2018. Available online: http://euanmearns.com/global-co2-emissions-forecast-to-2100/ (accessed on 7 June 2020).
38. Rochelle, C.A.; Czernichowski-Lauriol, I.; Milodowski, A.E. The impact of chemical reactions on CO_2 storage in geological formations: A brief review. *Geol. Soc. Spec. Publ.* **2004**, *233*, 87–106. [CrossRef]
39. Pan, Y.; Hui, D.; Luo, P.; Zhang, Y.; Sun, L.; Wang, K. Experimental Investigation of the Geochemical Interactions between Supercritical CO_2 and Shale: Implications for CO_2 Storage in Gas-Bearing Shale Formations. *Energy Fuels* **2018**, *32*, 1963–1978. [CrossRef]
40. Wan, J.; Tokunaga, T.K.; Ashby, P.D.; Kim, Y.; Voltolini, M.; Gilbert, B.; DePaolo, D.J. Supercritical CO_2 uptake by nonswelling phyllosilicates. *Proc. Natl. Acad. Sci. USA* **2018**, *115*, 873–878. [CrossRef]

41. Yin, H.; Zhou, J.; Xian, X.; Jiang, Y.; Lu, Z. Experimental study of the effects of sub- and super-critical CO_2 saturation on the mechanical characteristics of organic-rich shales. *Energy* **2017**, *132*, 84–95. [CrossRef]
42. Chiquet, P.; Broseta, D.; Thibeau, S. Wettability alteration of caprock minerals by carbon dioxide. *Geofluids* **2007**, *7*, 112–122. [CrossRef]
43. Ao, X.; Lu, Y.; Tang, J.; Chen, Y.; Li, H. Investigation on the physics structure and chemical properties of the shale treated by supercritical CO_2. *J. CO_2 Util.* **2017**, *20*, 274–281. [CrossRef]
44. Qin, C.; Jiang, Y.; Luo, Y.; Xian, X.; Liu, H.; Li, Y. Effect of Supercritical Carbon Dioxide Treatment Time, Pressure, and Temperature on Shale Water Wettability. *Energ. Fuel* **2017**, *31*, 493–503. [CrossRef]
45. Roshan, H.; Al-Yaseri, A.Z.; Sarmadivaleh, M.; Iglauer, S. On wettability of shale rocks. *J. Colloid Interface Sci.* **2016**, *475*, 104–111. [CrossRef]
46. Kaveh, N.S.; Barnhoorn, A.; Wolf, K.H. Wettability evaluation of silty shale caprocks for CO_2 storage. *Int. J. Greenh. Gas Control* **2016**, *49*, 425–435. [CrossRef]
47. Iglauer, S.; Al-yaseri, A.Z.; Rezaee, R.; Lebedev, M. CO_2 wettability of caprocks: Implications for structural storage capacity and containment security. *Geophys. Res. Lett.* **2015**, *42*, 9279–9284. [CrossRef]
48. Iglauer, S. CO_2-Water-Rock Wettability: Variability, Influencing Factors, and Implications for CO_2 Geostorage. *Acc. Chem. Res.* **2017**, *50*, 1134–1142. [CrossRef]
49. Schoemaker, C.; Barnhoorn, A.; van Hemert, P. Sorption and CT Experiments on the Transport and Sealing Properties of Samples Relevant to Key Sites. CATO2 Program, CATO2-WP3.3-D18; 2011; p. 52. Available online: https://www.CO2-cato.org/publications/library1/sorption-and-ct-experiments (accessed on 29 May 2020).
50. Lu, Y.; Chen, X.; Tang, J.; Li, H.; Zhou, L.; Han, S.; Ge, Z.; Xia, B.; Shen, H.; Zhang, J. Relationship between pore structure and mechanical properties of shale on supercritical carbon dioxide saturation. *Energy* **2019**, *172*, 270–285. [CrossRef]
51. Luo, X.; Ren, X.; Wang, S. Supercritical CO_2-water-shale interactions and their effects on element mobilization and shale pore structure during stimulation. *Int. J. Coal Geol.* **2019**, *202*, 109–127. [CrossRef]
52. Rezaee, R.; Saeedi, A.; Iglauer, S.; Evans, B. Shale alteration after exposure to supercritical CO_2. *Int. J. Greenh. Gas Control* **2017**, *62*, 91–99. [CrossRef]
53. Busch, A.; Alles, S.; Gensterblum, Y.; Prinz, D.; Dewhurst, D.N.; Raven, M.D.; Stanjek, H.; Krooss, B.M. Carbon dioxide storage potential of shales. *Int. J. Greenh. Gas Control* **2008**, *2*, 297–308. [CrossRef]
54. Chareonsuppanimit, P.; Mohammad, S.A.; Robinson, R.L.; Gasem, K.A.M. High-pressure adsorption of gases on shales: Measurements and modeling. *Int. J. Coal Geol.* **2012**, *95*, 34–46. [CrossRef]
55. Jiang, Y.; Luo, Y.; Lu, Y.; Qin, C.; Liu, H. Effects of supercritical CO_2 treatment time, pressure, and temperature on microstructure of shale. *Energy* **2016**, *97*, 173–181. [CrossRef]
56. Lahann, R.; Mastalerz, M.; Rupp, J.A.; Drobniak, A. Influence of CO_2 on New Albany Shale composition and pore structure. *Int. J. Coal Geol.* **2013**, *108*, 2–9. [CrossRef]
57. Zhou, D.; Zhang, G.; Wang, Y.; Xing, Y. Experimental investigation on fracture propagation modes in supercritical carbon dioxide fracturing using acoustic emission monitoring. *Int. J. Rock Mech. Min. Sci.* **2018**, *110*, 111–119. [CrossRef]
58. Goodman, A.; Sanguinito, S.; Tkach, M.; Natesakhawat, S.; Kutchko, B.; Fazio, J.; Cvetic, P. Investigating the role of water on CO_2-Utica Shale interactions for carbon storage and shale gas extraction activities- Evidence for pore scale alterations. *Fuel* **2019**, *242*, 744–755. [CrossRef]
59. Liu, F.; Lu, P.; Griffith, C.; Hedges, S.W.; Soong, Y.; Hellevang, H.; Zhu, C. CO_2-brine-caprock interaction: Reactivity experiments on Eau Claire shale and a review of relevant literature. *Int. J. Greenh. Gas Control* **2012**, *7*, 153–167. [CrossRef]
60. Lan, Q.; Xu, M.; Binazadeh, M.; Dehghanpour, H.; Wood, J.M. A comparative investigation of shale wettability: The significance of pore connectivity. *J. Nat. Gas Sci. Eng.* **2015**, *27*, 1174–1188. [CrossRef]
61. Burke, L.H.; Nevison, G.W.; Peters, W.E. Improved unconventional gas recovery with energized fracturing fluids: Montney example. In *SPE Eastern Regional Meeting*; Society of Petroleum Engineers: Columbus, OH, USA, 2011; pp. 316–325.
62. Hsu, S.C.; Nelson, P.P. Characterization of eagle ford shale. *Eng. Geol.* **2002**, *67*, 169–183. [CrossRef]
63. Morsy, S.; Sheng, J.J. Effect of Water Salinity on Shale Reservoir Productivity. *Adv. Pet. Explor. Dev.* **2014**, *8*, 9–14.

64. Li, Z.; Jiang, Z.; Yu, H.; Liang, Z. Organic matter pore characterization of the Wufeng-Longmaxi shales from the fuling gas field, Sichuan Basin: Evidence from organic matter isolation and low-pressure CO_2 and N2 adsorption. *Energies* **2019**, *12*, 1207. [CrossRef]
65. Armitage, P.J.; Faulkner, D.R.; Worden, R.H. Caprock corrosion. *Nat. Geosci.* **2013**, *6*, 79–80. [CrossRef]
66. Ozdemir, E.; Schroeder, K. Effect of moisture on adsorption isotherms and adsorption capacities of CO_2 on coals. *Energy Fuels* **2009**, *23*, 2821–2831. [CrossRef]
67. Jian, C.; Wenzhong, S.; Yihong, L. *Natural Product of Supercritical CO_2 Extraction*; Chemical Industry Press: Beijing, China, 2005.
68. Ross, D.J.K.; Bustin, R.M. The importance of shale composition and pore structure upon gas storage potential of shale gas reservoirs. *Mar. Pet. Geol.* **2009**, *26*, 916–927. [CrossRef]
69. Ma, Y.; Zhong, N.; Li, D.; Pan, Z.; Cheng, L.; Liu, K. International Journal of Coal Geology Organic matter/clay mineral intergranular pores in the Lower Cambrian Lujiaping Shale in the north-eastern part of the upper Yangtze area, China: A possible microscopic mechanism for gas preservation. *Int. J. Coal Geol.* **2015**, *137*, 38–54. [CrossRef]
70. Pfeifer, P.; Avnir, D. Chemistry in noninteger dimensions between two and three. *J. Chem. Phys.* **1983**, *79*, 3558–3565. [CrossRef]
71. Jarboe, P.J.; Candela, P.A.; Zhu, W.; Kaufman, A.J. Extraction of Hydrocarbons from High-Maturity Marcellus Shale Using Supercritical Carbon Dioxide. *Energy Fuels* **2015**, *29*, 7897–7909. [CrossRef]
72. Alemu, B.L.; Aagaard, P.; Munz, I.A.; Skurtveit, E. Caprock interaction with CO_2: A laboratory study of reactivity of shale with supercritical CO_2 and brine. *Appl. Geochem.* **2011**, *26*, 1975–1989. [CrossRef]
73. Nešić, S. Key issues related to modelling of internal corrosion of oil and gas pipelines—A review. *Corros. Sci.* **2007**, *49*, 4308–4338. [CrossRef]
74. Lyu, Q.; Ranjith, P.G.; Long, X.; Ji, B. Experimental investigation of mechanical properties of black shales after CO_2-water-rock interaction. *Materials* **2016**, *9*, 663. [CrossRef]
75. Lin, H.; Fujii, T.; Takisawa, R.; Takahashi, T.; Hashida, T. Experimental evaluation of interactions in supercritical CO_2/water/rock minerals system under geologic CO_2 sequestration conditions. *J. Mater. Sci.* **2008**, *43*, 2307–2315. [CrossRef]
76. Rempel, K.U.; Liebscher, A.; Heinrich, W.; Schettler, G. An experimental investigation of trace element dissolution in carbon dioxide: Applications to the geological storage of CO_2. *Chem. Geol.* **2011**, *289*, 224–234. [CrossRef]
77. Jean, J.S.; Wang, C.L.; Hsiang, H.I.; Li, Z.; Yang, H.J.; Jiang, W.T.; Yang, K.M.; Bundschuh, J. Experimental investigation of trace element dissolution in formation water in the presence of supercritical CO_2 fluid for a potential geological storage site of CO_2 in Taiwan. *J. Nat. Gas Sci. Eng.* **2015**, *23*, 304–314. [CrossRef]
78. Chen, Y.; Furmann, A.; Mastalerz, M.; Schimmelmann, A. Quantitative analysis of shales by KBr-FTIR and micro-FTIR. *FUEL* **2014**, *116*, 538–549. [CrossRef]
79. Lu, X.; Jin, D.; Wei, S.; Zhang, M.; Zhu, Q.; Shi, X.; Deng, Z.; Guo, W.; Shen, W. Competitive adsorption of a binary CO_2-CH4 mixture in nanoporous carbons: Effects of edge-functionalization. *Nanoscale* **2015**, *7*, 1002–1012. [CrossRef] [PubMed]
80. Wu, T.; Xue, Q.; Li, X.; Tao, Y.; Jin, Y.; Ling, C.; Lu, S. Extraction of kerogen from oil shale with supercritical carbon dioxide: Molecular dynamics simulations. *J. Supercrit. Fluids* **2016**, *107*, 499–506. [CrossRef]
81. Rao, D.N.; Girard, M.G. A new technique for reservoir wettability characterization. *J. Can. Pet. Technol.* **1996**, *35*, 31–39. [CrossRef]
82. Anderson, W.G. Wettability Literature Survey—Part 2: Wettability Measurement. *J. Pet. Technol.* **1986**, *38*, 1246–1262. [CrossRef]
83. Zhu, Z.; Li, M.; Lin, M.; Peng, B.; Sun, L.; Chen, L. Investigation on variations in wettability of reservoir rock induced by CO_2-brine-rock interactions. In *SPE EUROPEC/EAGE Annual Conference and Exhibition*; Society of Petroleum Engineers: Vienna, Austria, 2011; Volume 5, pp. 4027–4038.
84. Mitchell, A.G.; Hazell, L.B.; Webb, K.J. *Wettability Determination: Pore Surface Analysis*; Society of Petroleum Engineers: New Orleans, LA, USA, 1990; pp. 351–360.
85. Siddiqui, M.A.Q.; Ali, S.; Fei, H.; Roshan, H. Current understanding of shale wettability: A review on contact angle measurements. *Earth-Sci. Rev.* **2018**, *181*, 1–11. [CrossRef]
86. Liang, L.; Luo, D.; Liu, X.; Xiong, J. Experimental study on the wettability and adsorption characteristics of Longmaxi Formation shale in the Sichuan Basin, China. *J. Nat. Gas Sci. Eng.* **2016**, *33*, 1107–1118. [CrossRef]

87. Liang, L.; Xiong, J.; Liu, X. Journal of Natural Gas Science and Engineering Experimental study on crack propagation in shale formations considering hydration and wettability. *J. Nat. Gas Sci. Eng.* **2015**, *23*, 492–499. [CrossRef]
88. Xu, M.; Dehghanpour, H. Advances in understanding wettability of tight and shale gas formations. In *SPE Annual Technical Conference and Exhibition*; Society of Petroleum Engineers: Alberta, AB, Canada, 2014; Volume 7, pp. 5161–5179.
89. Mirchi, V.; Saraji, S.; Goual, L.; Piri, M. Dynamic interfacial tension and wettability of shale in the presence of surfactants at reservoir conditions. *Fuel* **2015**, *148*, 127–138. [CrossRef]
90. Yuan, W.; Li, X.; Pan, Z.; Connell, L.D.; Li, S.; He, J. Experimental investigation of interactions between water and a lower silurian chinese shale. *Energy Fuels* **2014**, *28*, 4925–4933. [CrossRef]
91. Odusina, E.; Sondergeld, C.; Rai, C. An NMR Study on Shale Wettability. In *SPE Canadian Unconventional Resources Conference*; Society of Petroleum Engineers: Alberta, AB, Canada, 2011.
92. Sun, Y.; Bai, B.; Wei, M. *Microfracture and Surfactant Impact on Linear Cocurrent Brine Imbibition in Gas-Saturated Shale*; Energy Fuels: Lakewood, CO, USA, 2015.
93. Roychaudhuri, B.; Tsotsis, T.T.; Jessen, K. An experimental investigation of spontaneous imbibition in gas shales. *J. Pet. Sci. Eng.* **2013**, *111*, 87–97. [CrossRef]
94. Lan, Q.; Ghanbari, E.; Dehghanpour, H.; Hawkes, R. Water Loss Versus Soaking Time: Spontaneous Imbibition in Tight Rocks. *Energy Technol.* **2014**, *2*, 1033–1039. [CrossRef]
95. Dehghanpour, H.; Lan, Q.; Saeed, Y.; Fei, H.; Qi, Z. Spontaneous imbibition of brine and oil in gas shales: Effect of water adsorption and resulting microfractures. *Energy Fuels* **2013**, *27*, 3039–3049. [CrossRef]
96. Makhanov, K.; Habibi, A.; Dehghanpour, H.; Kuru, E. Journal of Unconventional Oil and Gas Resources Liquid uptake of gas shales: A workflow to estimate water loss during shut-in periods after fracturing operations. *J. Unconv. Oil GAS Resour.* **2014**, *7*, 22–32. [CrossRef]
97. Arif, M.; Barifcani, A.; Lebedev, M.; Iglauer, S. Impact of Solid Surface Energy on Wettability of CO_2-brine-Mineral Systems as a Function of Pressure, Temperature and Salinity. *Energy Procedia* **2017**, *114*, 4832–4842. [CrossRef]
98. Arif, M.; Abu-Khamsin, S.A.; Iglauer, S. Wettability of rock/CO_2/brine and rock/oil/CO_2 -enriched-brine systems:Critical parametric analysis and future outlook. *Adv. Colloid Interface Sci.* **2019**, *268*, 91–113. [CrossRef]
99. Broseta, D. Assessing Seal Rock Integrity for CO_2 Geological Storage Purposes. In *Geomechanics in CO_2 Storage Facilities*; ISTE: Pau, France, 2013; pp. 3–20.
100. Pentland, C.H.; El-Maghraby, R.; Iglauer, S.; Blunt, M.J. Measurements of the capillary trapping of super-critical carbon dioxide in Berea sandstone. *Geophys. Res. Lett.* **2011**, *38*, L06401. [CrossRef]
101. Krevor, S.; Blunt, M.J.; Benson, S.M.; Pentland, C.H.; Reynolds, C.; Al-Menhali, A.; Niu, B. Capillary trapping for geologic carbon dioxide storage—From pore scale physics to field scale implications. *Int. J. Greenh. Gas Control* **2015**, *40*, 221–237. [CrossRef]
102. Andrew, M.; Bijeljic, B.; Blunt, M.J. Pore-scale contact angle measurements at reservoir conditions using X-ray microtomography. *Adv. Water Resour.* **2014**, *68*, 24–31. [CrossRef]
103. Chaudhary, K.; Guiltinan, E.J.; Cardenas, M.B.; Maisano, J.A. Wettability measurement under high P-T conditions using X-ray imaging with application to the brine-supercritical CO_2 system. *Geochem. Geophys. Geosyst.* **2015**, *16*, 2858–2864. [CrossRef]
104. Bikkina, P.; Shaik, I. *Interfacial Tension and Contact Angle Data Relevant to Carbon Sequestration*; IntechOpen: London, UK, 2018.
105. Feng, G.; Kang, Y.; Sun, Z.D.; Wang, X.C.; Hu, Y.Q. Effects of supercritical CO_2 adsorption on the mechanical characteristics and failure mechanisms of shale. *Energy* **2019**, *173*, 870–882. [CrossRef]
106. Madland, M.V.; Finsnes, A.; Alkafadgi, A.; Risnes, R.; Austad, T. The influence of CO_2 gas and carbonate water on the mechanical stability of chalk. *J. Pet. Sci. Eng.* **2006**, *51*, 149–168. [CrossRef]
107. Bennion, D.B.; Bachu, S. Drainage and imbibition relative permeability relationships for supercritical CO_2/brine and H2S/brine systems in intergranular sandstone, carbonate, shale, and anhydrite rocks. *SPE Reserv. Eval. Eng.* **2008**, *11*, 487–496. [CrossRef]
108. Farquhar, S.M.; Pearce, J.K.; Dawson, G.K.W.; Golab, A.; Sommacal, S.; Kirste, D.; Biddle, D.; Golding, S.D. A fresh approach to investigating CO_2 storage: Experimental CO_2-water-rock interactions in a low-salinity reservoir system. *Chem. Geol.* **2015**, *399*, 98–122. [CrossRef]

109. Rutqvist, J.; Vasco, D.W.; Myer, L. Coupled reservoir-geomechanical analysis of CO_2 injection and ground deformations at In Salah, Algeria. *Int. J. Greenh. Gas Control* **2010**, *4*, 225–230. [CrossRef]
110. Rutqvist, J.; Wu, Y.; Tsang, C.; Bodvarsson, G. A modeling approach for analysis of coupled multiphase fluid flow, heat transfer, and deformation in fractured porous rock. *Int. J. Rock Mech. Min. Sci.* **2002**, *39*, 429–442. [CrossRef]
111. Aziz, N.I.; Ming-Li, W. The effect of sorbed gas on the strength of coal—An experimental study. *Geotech. Geol. Eng.* **1999**, *17*, 387–402. [CrossRef]
112. Viete, D.R.; Ranjith, P.G. The effect of CO_2 on the geomechanical and permeability behaviour of brown coal: Implications for coal seam CO_2 sequestration. *Int. J. Coal Geol.* **2006**, *66*, 204–216. [CrossRef]
113. Ranathunga, A.S.; Perera, M.S.A.; Ranjith, P.G.; Bui, H. Super-critical CO_2 saturation-induced mechanical property alterations in low rank coal: An experimental study. *J. Supercrit. Fluids* **2016**, *109*, 134–140. [CrossRef]
114. Ranathunga, A.S.; Perera, M.S.A.; Ranjith, P.G. Influence of CO_2 adsorption on the strength and elastic modulus of low rank Australian coal under confining pressure. *Int. J. Coal Geol.* **2016**, *167*, 148–156. [CrossRef]
115. Perera, M.S.A.; Ranjith, P.G.; Viete, D.R. Effects of gaseous and super-critical carbon dioxide saturation on the mechanical properties of bituminous coal from the Southern Sydney Basin. *Appl. Energy* **2013**, *110*, 73–81. [CrossRef]
116. De Jong, S.M.; Spiers, C.J.; Busch, A. International Journal of Greenhouse Gas Control Development of swelling strain in smectite clays through exposure to carbon dioxide. *Int. J. Greenh. Gas Control* **2014**, *24*, 149–161. [CrossRef]
117. Zhang, D.; Ranjith, P.G.; Perera, M.S.A. The brittleness indices used in rock mechanics and their application in shale hydraulic fracturing: A review. *J. Pet. Sci. Eng.* **2016**, *143*, 158–170. [CrossRef]
118. Modahl, I.S.; Nyland, C.A.; Raadal, H.L.; Kårstad, O.; Torp, T.A.; Hagemann, R. Life cycle assessment of gas power with CCS—A study showing the environmental benefits of system integration. *Energy Procedia* **2011**, *4*, 2470–2477. [CrossRef]
119. Khoo, H.H.; Tan, R.B.H. Life cycle investigation of CO_2 recovery and sequestration. *Environ. Sci. Technol.* **2006**, *40*, 4016–4024. [CrossRef]
120. Bauer, C.; Heck, T.; Dones, R.; Mayer-Spohn, O.; Blesl, M. NEEDS (New Energy Externalities Developments for Sustainability). In *Final Report on Technical Data, Costs, and Life Cycle Inventories of Advanced Fossil Power Generation Systems*; Paul Scherrer Institut (PSI): Villigen, Switzerland, 2009.
121. Viebahn, P.; Nitsch, J.; Fischedick, M.; Esken, A.; Schüwer, D.; Supersberger, N.; Edenhofer, O. Comparison of carbon capture and storage with renewable energy technologies regarding structural, economic, and ecological aspects in Germany. *Int. J. Greenhouse Gas Control* **2007**, *1*, 121–133. [CrossRef]
122. Schreiber, A.; Zapp, P.; Kuckshinrichs, W. Environmental assessment of German electricity generation from coal-fired power plants with amine-based carbon capture. *Int. J. Life Cycle Assess.* **2009**, *14*, 547–559. [CrossRef]
123. Korre, A.; Nie, Z.; Durucan, S. Life cycle modelling of fossil fuel power generation with post-combustion CO_2 capture. *Int. J. Greenh. Gas Control* **2010**, *4*, 289–300. [CrossRef]
124. Marx, J.; Schreiber, A.; Zapp, P.; Haines, M.; Hake, J.F.; Gale, J. Environmental evaluation of CCS using Life Cycle Assessment—A synthesis report. *Energy Procedia* **2011**, *4*, 2448–2456. [CrossRef]
125. IEA. Greenhouse Gas R&D Programme (IEA GHG): Environmental Impact of Solvent Scrubbing of CO_2. 2006. Available online: https://ieaghg.org/docs/General_Docs/Reports/2006-14%20Environmental%20Impact%20of%20Solvent%20Scrubbing%20of%20CO2.pdf (accessed on 29 May 2020).
126. Bradshaw, J.; Bachu, S.; Bonijoly, D.; Burruss, R.; Holloway, S.; Christensen, N.P.; Mathiassen, O.M. CO_2 storage capacity estimation: Issues and development of standards. *Int. J. Greenh. Gas Control* **2007**, *1*, 62–68. [CrossRef]
127. Bachu, S.; Bonijoly, D.; Bradshaw, J.; Burruss, R.; Holloway, S.; Christensen, N.P.; Mathiassen, O.M. CO_2 storage capacity estimation: Methodology and gaps. *Int. J. Greenh. Gas Control* **2007**, *1*, 430–443. [CrossRef]
128. Yun, Y. *Recent Advances in Carbon Capture and Storage*; Janeza Trdine 9, 51000; IntechOpen: London, UK, 2017. [CrossRef]
129. Tayari, F.; Blumsack, S.; Dilmore, R.; Mohaghegh, S.D. Techno-economic assessment of industrial CO_2 storage in depleted shale gas reservoirs. *J. Unconv. Oil Gas Resour.* **2015**, *11*, 82–94. [CrossRef]

130. Jia, B.; Tsau, J.S.; Barati, R. A review of the current progress of CO_2 injection EOR and carbon storage in shale oil reservoirs. *Fuel* **2019**, *236*, 404–427. [CrossRef]
131. Bielicki, J.M.; Langenfeld, J.K.; Tao, Z.; Middleton, R.S.; Menefee, A.H.; Clarens, A.F. The geospatial and economic viability of CO_2 storage in hydrocarbon depleted fractured shale formations. *Int. J. Greenh. Gas Control* **2018**, *75*, 8–23. [CrossRef]
132. Hoel, M.; Jensen, S. Cutting costs of catching carbon-Intertemporal effects under imperfect climate policy. *Resour. Energy Econ.* **2012**, *34*, 680–695. [CrossRef]
133. Durmaz, T. The economics of CCS: Why have CCS technologies not had an international breakthrough? *Renew. Sustain. Energy Rev.* **2018**, *95*, 328–340. [CrossRef]
134. Smith, L.A.; Gupta, N.; Sass, B.M.; Bubenik, T.A.; Byrer, C.; Bergman, P. Engineering and Economic Assessment of Carbon Dioxide Sequestration in Saline Formations. In Proceedings of the National Conference on Carbon Sequestration, Washington, DC, USA, 15–17 May 2001.
135. Heddle, G.; Herzog, H.J.; Klett, M. *The Economics of CO_2 Storage*; Massachusetts Institute of Technology Laboratory for Energy and the Environment: Massachusetts, MA, USA, 2003.
136. Rubin, E.S.; Rao, A.B.; Chen, C. Comparative assessments of fossil fuel power plants with CO_2 capture and storage. *Greenh. Gas Control Technol.* **2005**, *7*, 285–293.
137. Holloway, S. Sequestration—The Underground Storage of Carbon Dioxide. In *Climate Change and Energy Pathways for the Mediterranean*; Moniz, E.J., Ed.; Springer: Dordrecht, The Netherlands, 2008; pp. 61–88.
138. Finkenrath, M. Cost and Performance of Carbon Dioxide Capture from Power Generation. *IEA Energy Pap.* **2012**, *35*, 51. [CrossRef]
139. Lafforgue, G.; Magné, B.; Moreaux, M. Energy substitutions, climate change and carbon sinks. *Ecol. Econ.* **2008**, *67*, 589–597. [CrossRef]
140. REN21. *Renewables 2017 Global Status Report*; Technical report; Renewable Energy Policy Network for the 21st Century: Paris, France, 2017.